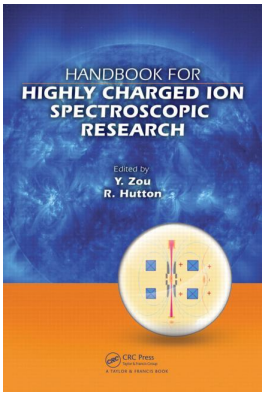

Handbook for Highly Charged Ion Spectroscopic Research

Zou Yaming, Hutton Roger

Spectroscopic Instruments

Publication details
https://www.routledgehandbooks.com/doi/10.1201/b11319-5
Hutton Roger, Shi Zhan, Martinson Indrek
Published online on: 20 Sep 2011

3

Spectroscopic Instruments

Roger Hutton, Zhan Shi, and Indrek Martinson

CONTENTS

3.1 Introduction

The term "spectrometer" refers to any energy-resolving instrument; however, in this chapter we will concentrate on photon energy-resolving instruments or, to be more specific, wavelength-dispersive instruments. The basic theme of this chapter concerns techniques for the study of highly charged ions (HCIs), and one aspect of this should be their spectra. Spectra from HCIs

can cover very large ranges in photon energy, or wavelength, that is, from over 100 keV photons for H-like resonance lines in very-highly charged ions to less than 1 eV photons for hyperfine transitions. For example, the 1*s* hyperfine splitting gives a transition at 3858.2260 ± 0.30 Å (3.2 eV) in $^{203}Tl^{80+}$ [1], whereas the 1*s* to 2*p* resonance transitions have energies more than 90 keV (simple *Z* scaling). Another example is provided by transitions in highly ionized iron. The resonance transitions in He-like iron, Fe XXV (from $n = 2$ to $n = 1$), occur in the x-ray region, at 1.85 Å, or 6.7 keV. These lines have been observed in solar flares and in tokamaks [2]. In Al-like Fe XIV, there is a forbidden M1 transition within the $3s^2 3p^2 P$ ground term, a strong line in the solar corona, at 5303 Å. Already in 1945, Edlén [3] had identified 23 such corona lines, in highly charged Ar, Ca, Fe, and Ni, with wavelengths ranging from 3328 to 10,797 Å. The unit Å is not an official SI unit but is named after the Swedish physicist Ångström and is equal to 10^{-10} m, that is, 0.1 nm.

Excited energy levels in an HCI, A^{q+}, decay by electronic transitions, resulting in the emission of electromagnetic radiation. However, nonradiative transitions to the ground state, or to some excited state in the next ion $A^{(q+1)+}$ by electron emission, are sometimes also energetically possible. To determine excitation energies and energy differences in ions, both photon and electron spectroscopies are therefore applicable. In this chapter, the emphasis is placed, as said above, on photon spectroscopy of multiply ionized atoms. This is often called classical spectroscopy, which may sound a bit old-fashioned. However, it can often be the only possible way for experimental studies of spectra and structures of HCIs, for instance, when investigating solar and stellar spectra or hot thermonuclear fusion plasmas.

As the energy, and so the wavelength, region covers a very large range, a variety of spectrographs and spectrometers will be needed. For instance, in He-like boron, B IV, 141 spectral lines have been observed between 43 and 4813 Å [4]. In a famous and pioneering paper, Edlén and Swings [5] studied the Fe III spectrum between 500 and 6500 Å and observed 1500 spectral lines in this region. They classified all these lines which resulted in 320 new energy levels for Fe III, which are of great importance in astrophysics.

It will be seen in the following that a number of optical techniques will be needed to cover such large ranges in photon energies. Basically, three wavelength regions can be defined where different techniques must be used. They are (i) from infrared down to about 1850 Å, (ii) 1850 Å down to around 10 Å, and (iii) below 10 Å. Each of these regions and their peculiarities will be discussed below.

Before discussing the three regions defined above, a few general remarks about photon spectrometers and other instruments used in photon spectroscopy are called for.

3.2 General about Spectroscopic Instruments

The group of the so-called classical spectroscopic instruments can be divided between those with prisms and those with gratings. Of these, the latter are dominant, especially when HCIs are being studied because of their limited useful wavelength region for prism-based instruments. There are also several types of interferometers, often used in the so-called Fourier transform spectroscopy. Such instruments are very important for accurate atomic and molecular studies, but so far have seen limited applications in the case of multiply ionized atoms.

For the instruments to be discussed here, we can distinguish some special chief outlines. In a typical spectrometer, the light to be studied enters the instrument through an entrance slit in the focal plane of a spherical mirror or grating. In the case of the mirror, the divergent bundle of light will be made parallel by the collimator lens or spherical mirror and sent to a grating as dispersing element and then to a focusing mirror which forms an image of the entrance slit in the focal plane. The rays leave the grating with angles which depend on the wavelengths, and hence the position of the image of the entrance slit is a function $x(\lambda)$ of the wavelength.

Photographic emulsion was the dominating detector for spectroscopic instruments for many years. It has several good properties thanks to which it can still be used. Among the good properties are the integrating capability, the two-dimensional registration with high resolution, storage of the signal directly in the detector with high information density, and practically unlimited storage time. The data storage capacity of a photographic plate should not be mocked. Twenty years ago, or so, data were recorded on 9 in. floppy discs but who can read such things now! Among the disadvantages, the most serious one is the highly nonlinear response to light intensity. Moreover, the sensitivity is lower than that for photoelectrical detection and the emulsions are not generally sensitive to single-photon events. This method of photon detection misses any time variation of the light intensity, and photographic emulsion can thus be described as a detector of illumination. Photographic plates have been almost exclusively replaced by either micro-channel plates (MCPs), detectors (see Chapter 6), or charge-coupled device (CCD)-based detectors (see Chapter 5).

There are several designations and names for spectroscopic instruments which are sometimes used without any accurate distinction. A spectrograph usually means an instrument with a photographic plate in the spectral image plane, sometimes recording a large range of wavelengths simultaneously. Nowadays, photographic plates are often replaced by electronic array detectors as mentioned in the previous paragraph. The term "monochromator" means that a single-exit slit is used to select a spectral line or a narrow spectral band. We can also have a scanning monochromator, by rotating the

disperser (for instance, a grating) which can thus also be called as a scanning spectrometer.

Spectroscopic instruments for different wavelength ranges are constructed according to different principles. Thus, spectrographs for photographic registration can only be used for wavelengths below 11,000 Å. Furthermore, because of reduced reflectivity, at low angles of incidence, for all materials and for wavelengths shorter than 1000–1500 Å (see Figure 3.1), reflections should usually be minimal, that is, only one. Below 300 Å, one really must apply grazing incidence methods for this single reflection as the reflectivity for all materials increases with the incidence angle. Readers may demonstrate this to themselves using the XOP software [6]. XOP is a freely downloadable set of software which performs the calculation of the reflectivity of many materials as a function of incidence angle, photon energy, surface roughness, and so on. Because of transmission problems, it is also necessary to eliminate air (and thus measure in vacuum) when radiation below 2000 Å is observed, that is, the vacuum UV region. Figure 3.2 shows an example calculated using XOP. It is for the reflection of 1000 Å photons from a gold surface as a function of angle (given in milliradians) and measured from the surface (i.e., not from the normal). The surface is assumed to be perfectly smooth, but roughness can be dealt with by the software.

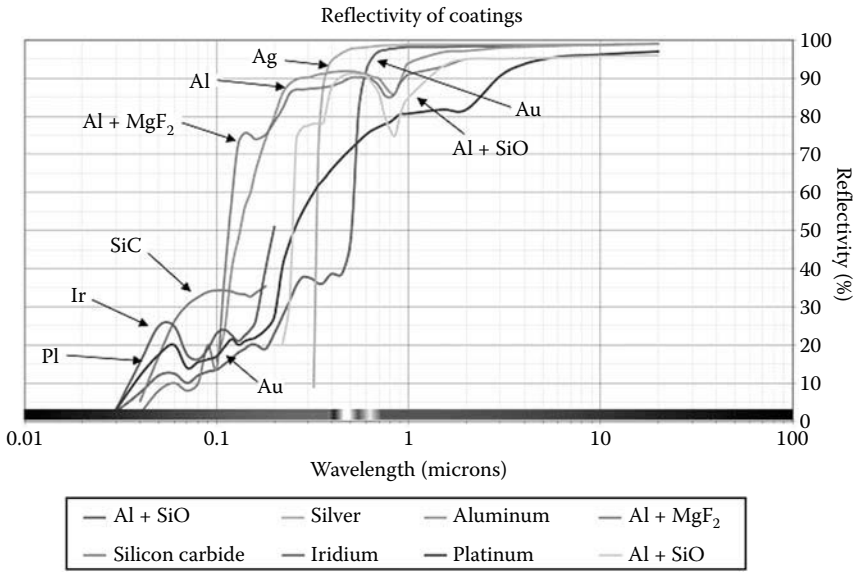

FIGURE 3.1
Reflectivity for a number of common mirror coatings as a function of wavelength (μm) at normal incidence, that is, light incident along (or close to the normal of the optical component). (Courtesy of McPherson Inc., Massachusetts, USA [7].)

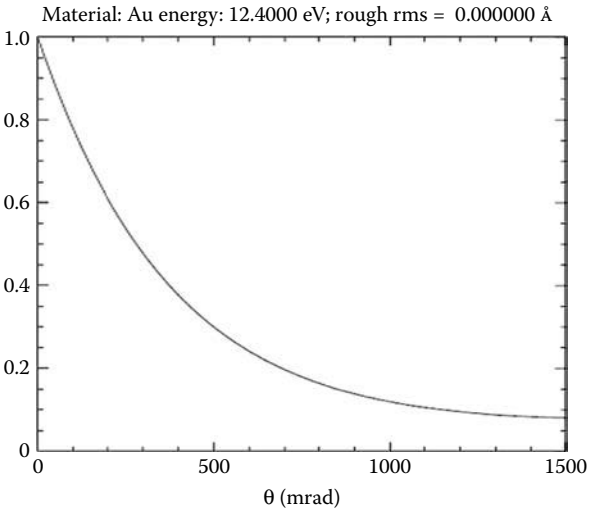

FIGURE 3.2
Reflection of 1000 Å photons from a gold surface as a function of angle (given in milliradians) and measured from the surface (i.e., not from the normal). The surface is assumed to be perfectly smooth in this case.

Not only does the wavelength region influence the construction of a spectroscopic instrument, but also the width of the region in which one would like to work with a certain instrument. Those who want to study the hyperfine structure of a certain spectral line will often select a laser spectroscopic method. For term analysis, where many spectral lines are needed, a variety of instruments may be required. Out of interest, the region below 1850 Å and down to around 100 Å is often called the vacuum ultraviolet region. There are three underlying reasons for this change at around 1850 Å: (i) the absorption of quartz, (ii) the absorption of oxygen, and (iii) more of historic interest, the absorption of the gelatin in standard photographic plates.

3.3 Diffraction Gratings

With the exception of interferometers, almost all spectroscopic instruments use reflective gratings as the dispersive element. However, the first gratings to be produced were of the transmission type and were constructed by the American astronomer D. Rittenhouse in 1785. Rittenhouse (1732–1796) was viewing a distant light source through a fine silk handkerchief. He then made up a square of parallel hairs and found that red light was bent more than blue light. In the early nineteenth century, the German physicist Joseph von Fraunhofer (1787–1826) discovered the dark lines in the Sun's

spectrum, now known as Fraunhofer lines. He was also the first scientist to extensively use diffraction gratings, which he himself made on glass or metal surfaces. It is considered that his work set the stage for the development of spectroscopy. Somewhat more modern diffraction gratings were first developed by the American physicist Henry A. Rowland (1848–1901). He also invented the concave grating, which could replace prisms and plane gratings and revolutionized spectrum analysis. Around 1882, he managed to construct a machine which could engrave as many as 20,000 lines/in. (785 lines/mm) for diffraction gratings. He then ruled on spherical concave surfaces, thus eliminating the need for additional lenses and mirrors in spectrometers and used them to develop exact spectrometry. Later developments were made at the Massachusetts Institute of Technology (MIT) and also by the company Bausch and Lomb and others [8].

From 1965, a new technique of grating production has been developed. This is the holographic method, which produces gratings by recording interference fringes on photosensitive materials. This procedure results in the grove spacing being absolutely constant, and the gratings are therefore free of ghosts. The efficiency is, however, lower than that of ruled gratings.

From the mid-1980s, a new form of diffraction grating became available, the so-called aberration-corrected flat-field grating. These were originally produced by Hamamatsu using a mechanical ruling device but more recently have been manufactured using holographic techniques, for example, those produced by Jobin Yvon [9]. Note that Yvon, along with a number of other companies, provided excellent online guides and details of grating design, use, and technology.

3.4 Spectrometer Slits

Before discussing the effect of slits on the performance of a spectroscopic instrument, it is interesting to think about why spectral features are most often lines.

A line is called a line just because it is the line-shaped image of the line-shaped slit in the focal plane of the spectrometer. And that is how it looked on a photographic plate. It is interesting to notice how things change with time. For some time, and in almost all "modern" instruments, a spectral line was just the photon or light intensity distribution as a function of wavelength. But currently, most instruments use CCDs or other imaging detectors, so now the lines look like lines again, in the original sense. One can also ask whether other shapes for the entrance aperture could be used. Newton used a circular opening in his first prism experiment, but as soon as one thinks of trying to separate spectral features, like, for example, Fraunhofer did, then you need the smallest possible extension of the input aperture in the dispersion direction. But it does not matter if the aperture is wide in the perpendicular

direction. A very small dot would be difficult to see directly with the eye in the early instruments and also later when photographic plates began to be used. However, circular apertures are fine for use in combination with CCD detectors, except now lines become spots. The use of circular apertures has great implications, for example, in the design of echelle-based spectrometers (see Section 3.7.2).

3.5 Entrance Slit

Whether a spectrometer has two slits or one is depending on whether it is designed to be a monochromator or a spectrograph. In either case, the width of the slit (or slits) plays an important role in defining the characteristics of the instrument. The most obvious function is that the entrance slit will limit the amount of light, not only intensity but more importantly angular direction, entering the spectrometer.

The width of the entrance slit may also be the defining factor for the resolution of the spectrometer. Basically, the optics in a spectrometer is designed to image the entrance slit, usually in a one-to-one manner on the spectral image plane. If the width of the slit is smaller than the diffraction limited image of the optics, then the slit does not define the resolution and the resolution will be diffraction-limited. If the width of the entrance slit is greater than the diffraction-limited image, then the resolution is defined by the width of the entrance slit.

The instrument profile of a spectrograph is given by the convolution of the slit function and the diffraction profile defined by the aperture of the dispersive element (grating). In the case of a monochromator, the instrument profile must include the exit slit function as part of the convolution. Although the role of exit slits has been greatly reduced in recent years, due to the increasing use of multichannel detection techniques, it is still useful to look at the role of an exit slit. One of the roles of an exit slit is to limit the amount of light falling onto the detector, in the case of single-channel detection. A little argument will show that the optimal width of the exit slit is exactly the same width as the entrance slit.

First consider the case where diffraction can be ignored and look at the influence of the entrance and exit slits. If we assume that the entrance slit has a width a_1 and luminance (see below for a definition) B, then we can describe the slit as a rectangle. We can also assume that the exit slit can be defined by a width a_2 and a transmission = 1 over the slit width and 0 outside. If we ignore diffraction and aberration, then the convolution can be seen as a scanning of the exit slit over the entrance slit. Hence the flow of light onto a detector will be proportional to the total area presented by the two slits and this area changes during the scanning (convolution). There are two situations to consider: (i) the entrance slit is narrower than the exit slit, and (ii) the entrance slit is the

broadest. However, the optimal appears when $a_1 = a_2$ and where the slits lead to a triangular instrument profile.

Luminance describes the amount of light that passes through or is emitted from a particular area, and falls within a given solid angle. It is an invariant in geometrical optics, that is, if a light bundle is hard focused, then it will appear as though the spot is brighter, but the solid angle will also be larger, so the luminance in constant (except for absorption at lenses, etc.). This is an important concept in optics and is similar to the idea of emittance in ion beam optics.

3.6 Aberrations

No discussion of spectrometers would be complete without a mention of aberrations, as in the end it is often these that limit resolution or light collection. The easiest way to approach aberration studies for a particular instrument is through ray tracing. Here free downloadable software such as Zmax or Shadow can be used. The most common aberrations when discussing spectrometers are spherical aberration and astigmatism. Below we will discuss these aberrations from Seidel theory. The basis of this is to take the next higher-order approximation to the theory of geometrical optics. Geometrical optics, or Gaussian theory of image formation, works in the region when the so-called paraxial rays are considered, that is, $\sin\alpha = \tan\alpha = \alpha$. The next order of approximation is given by letting $\sin\alpha = \alpha - \alpha^3/3!$ and $\tan\alpha = \alpha + \alpha^3/3!$ Doing this allows the construction of a third-order theory of image formation which takes into account nonparaxial rays. The deviations from perfect imaging will be the Seidel aberrations, of which spherical aberration and astigmatism are just two of the terms. There are five Seidel terms, each representing a different form of aberration and each term is a complex function of the position in the object and image planes, the radius of curvature of the optical element, and also the refractive index (if needed). The five Seidel terms were first defined and developed in the original article by Seidel in 1856 [10]. Spherical aberration refers to the fact that even light from an infinitely distant object will not be focused to a point by a spherical mirror. This is caused by the fact that light rays are reflected with a larger angle by the outer parts of a mirror compared to those from the inner mirror region.

Like all aberrations, this is best studied using ray-tracing techniques. However, an interesting measure of the importance of spherical aberration is the circle of least confusion. Here, a comparison can be made between the size of the circle of least confusion and the size of the image due to diffraction. This can be done by comparing the two terms below:

$\Delta_{SA} = h^3/8f^2$, which gives the size of the circle of least confusion and
$\Delta_R = \lambda f/2h$, which gives the diffraction-limited image size.

Here, h is the height of the light rays from the optical axis (i.e., the mirror radius), f the focal length, and λ the wavelength.

As an example, a mirror with $f = 3\,\text{m}$ and $h = 6.5\,\text{cm}$ gives $\Delta_{SA} = 4\,\mu\text{m}$, whereas a mirror with the same radius but $f = 1.5\,\text{m}$ has $\Delta_{SA} = 16\,\mu\text{m}$. For 5000 Å wavelength photons, the values of Δ_R are 12.5 and 6 μm for the 3 and 1.5 m mirrors, respectively. Hence the spatial resolution of the 3 m mirror is limited by diffraction, whereas for the 1.5 m mirror it is by spherical aberration.

Another aberration that should be mentioned as of importance to spectrometer is astigmatism. Astigmatism leads to a point object not being imaged as a point. There will be two positions where the image will be a straight line and the lines are perpendicular to each other. The distance between the two focus positions is given by the Seidel theory as hy^2, where y is the distance of the object from the optical axis. This aberration limits the useful height of spectrometer entrance slits, for example. Seidel theory was developed for normal, or close to normal incidence. The size of most aberrations increase as a function of the incidence angle, which is particularly true for astigmatism. Grazing incidence spectrometers are very limited in both entrance slit height and grating width by aberrations. For a full discussion of this, see the work of Mack et al. [11]. In particular, astigmatism will limit the useful grating size and hence the light collection angle for very high incidence angles. This has to be weighted against the increase in reflectivity as a function of incidence angle for wavelengths below 1000–1500 Å when choosing spectrometer geometry (see Section 3.8). Before leaving this short discussion on aberrations, we should mention coma. This aberration comes about when imaging a point that does not lie on the optical axis. The importance of coma can be judged by the Seidel expression h^2y, where h and y are as above. Coma is particularly irritating in spectroscopic instruments because it will lead to asymmetric line shapes and all the problems incorporated with this. A full account of aberrations and their influence on optical systems can be found in the book by Welford [12]. As mentioned a number of times in this chapter, the way to estimate the importance of aberrations on the performance of an optical instrument is through ray-tracing.

3.7 Plane Grating Mounts

In spectrometers that employ plane gratings, the grating only performs the task of dispersing the light depending on wavelength. Focusing, and so on is done by auxiliary optical components. Hence wavelength dispersion and focusing can be optimized independently and this leads to plane grating spectrometers usually having higher light gathering properties. Plane grating spectrometers are usually more flexible than instruments using curved gratings as the grating can be changed without changing the optical properties.

Hence, it is often recommended to use plane grating instruments whenever it is possible. A number of mountings for plane gratings exist and some will be discussed below.

3.7.1 Czerny-Turner Mounting

One of the biggest advantages of this mounting is that coma can be totally eliminated, at least in the meridian plane.

The basic optics of this instrument is quite straightforward and it is relatively easy to understand how coma can be eliminated. The coma introduced by the collimating mirror, C, is equal and opposite in sign to that introduced by the focusing mirror, E (see Figure 3.3).

There are other mounts for plane gratings, for example, the Ebert and Eagle mounting, which can be described in the book by Samson and Ederer [13].

3.7.2 Echelle Mounting

In recent years, echelle gratings have become more popular in the construction of spectroscopic instruments. The main reasons for this are the developments in two-dimensional photon detectors such as MCPs and CCD-based detectors. An echelle grating acts more like an interferometer than a grating and works in a very high order of diffraction (see Figure 3.4).

Although echelle gratings offer very high wavelength dispersion, they give rise to very low divergence. Hence the most common way to use echelle gratings is with a cross-disperser, which can be either a grating or prism. For work below, the transmission cut-off of quartz at about 1850 Å gratings must be used. An interesting solution for an echelle cross-disperser geometry was given in 1958 by Harrison [8]. In Section 3.8, we will develop the idea of the Rowland circle. However, there is a second solution to the imaging properties of concave gratings, the so-called Wadsworth solution. This

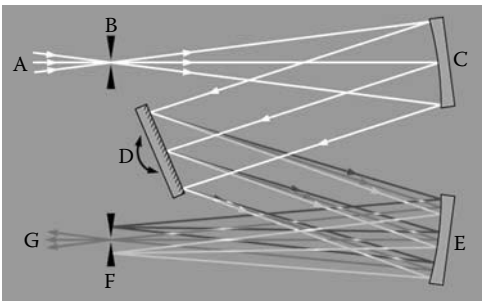

FIGURE 3.3
This shows one of the schemes for using a plane grating, the so-called CzernyTurner mounting.

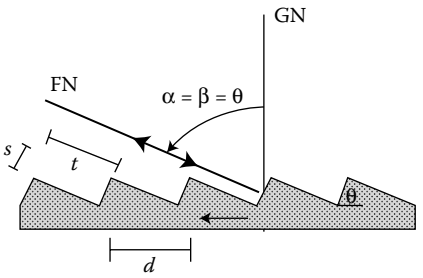

FIGURE 3.4
This shows the operation of an echelle grating. GN is the grating normal, FN the face normal, and d is the groove spacing.

geometry is very suited to work with an echelle grating. As will be shown in the section below, this solution requires the object to be at an infinite distance from the grating and the spectrum will be imaged along the direction of β (diffraction angle) $= 0$ and on a curved surface given as $r' = R/(1 + \cos\alpha)$, where R is the radius of curvature of the grating and α the angle of incidence. The mounting of an echelle grating requires parallel light impinging on the grating from an angle. The reflected and dispersed light will also be a parallel beam, hence the match with the Wadsworth mounting of the cross-disperser. The final spectrum will be two-dimensional with the cross-disperser throwing the different orders from the echelle ideally by just the height of the entrance slit. An example of such an instrument is described in the following section.

As we will see in the following section, the development of the focusing properties of a concave grating led to a number of conditions that must be fulfilled. One being the grating equation which tells in which direction a given wavelength will be focused, but not where. The following equation tells where the light at a given wavelength will be focused:

$$\cos\alpha\left(\frac{\cos\alpha}{r} - \frac{1}{R}\right) + \cos\beta\left(\frac{\cos\beta}{r'} - \frac{1}{R}\right) = 0,$$

where r is the object distance, r' the image distance, and R the radius of curvature.

One solution is to let the light source be at an infinite distance, that is, $r = \infty$, which is the same as using parallel light to fall on the echelle and also β (the diffraction angle) $= 0$. The spectrum will then fall on a surface given by $r' = R/(1 + \cos\alpha)$. This is known as the Wadsworth mounting of a concave grating.

As an example, we will consider the design of an echelle-based spectrometer where the wavelength resolution should be around 0.1 Å and the working range from 1500 to 6000 Å. Also we will consider that the instrument should be compact for convenience. A further important parameter in the design of

echelle spectrometers is the height of the object, as this defines how far each echelle order needs to be "thrown" to get good order sorting. In the example here, the object was an ion beam of 3 mm in diameter. Hence the entrance slit was chosen to be 3 mm in height. Using CCD detectors, there is no longer any reason why a slit is needed and circular apertures can be used. Such an instrument will be briefly mentioned below but we can mention here that it is very important to match the spectrometer to the properties of both the light source and detector. Most likely the optical components are going to be the cheapest part of any spectrometer.

For example, here 1 m radius of curvature optics are chosen. The line density of the echelle grating is fixed once the design criteria of the instrument are specified. It is surprising how little the choice is to the designer in fact. The free spectral range of an echelle grating is given by $\lambda^2/(2d \sin\theta)$, where d is the groove separation and θ the blaze angle. The plate factor, that is, the number of Å per mm, along an echelle order is $\lambda/R \tan\theta$, where R is the radius of curvature of the concave grating (and most likely the collimating concave mirror too). The plate factor is directly related to the required resolution and the properties of the detector. If we choose, for example, 2 Å/mm at 4000 Å, then the blaze angle is determined as we specified $R = 1$ m. The blaze angle should be 63°. If we choose the maximum length of the echelle order contains 4000 Å, this determines the echelle line spacing to be around 31 lines/mm. These parameters are very close to those of some commercially produced echelle gratings, for example, blaze angle of 63.26° and 31.6 lines/mm. The order sorting concave grating is now basically fixed by the detector dimensions. The instrument was required to work up to 6000 Å, so based on CCD chip of 25 mm length, we can require the echelle order containing 6000 Å to be, say 21 mm, in length and a free spectral range of 63 Å. We now require the plate factor of the order sorter to be $\lambda f r s$/slit height. This leads to a groove density of around 1100 lines/mm at 6000 Å and the spectrometer is completely specified.

3.8 Concave Grating Mounts

The geometry of plane grating mountings requires at least three reflections, collimation, dispersion, and finally focus. Such a spectrometer operating at short wavelength and at normal incidence, that is, the incident angle being less than around 10°, would have very bad efficiency due to the low reflectivity of all materials for wavelengths shorter than 1000–1500 Å (see Figure 3.1). For example, 20% of 20% of 20% would be a reflectivity of 0.8%. Hence mountings of gratings where the number of reflections can be minimized and preferably only one are highly useful, which shows the importance of concave grating. For wavelengths below 300 Å, the one "allowed" reflection must be at grazing incidence as reflectivity increases at higher angles of incidence. Of course,

there is a price to pay for the increased efficiency and that is the inability to compensate for aberrations. In particular, astigmatism is high for concave grating-based spectrometers.

Most mountings of concave gratings are based on the so-called Rowland circle geometry which will be introduced below. A full derivation of the results that will be presented here can be found in the work of Beutler [14].

3.8.1 Rowland Circle

The imaging properties of the concave grating can be understood via the following arguments. First, we define a co-ordinate system as in Figure 3.5: A$(x, y, 0)$ is the position of an object in the $z = 0$ plane and B$(x', y', 0)$ is the position of the image after diffraction by the grating. P(u, w, l) is any point on the grating surface and O is the centre of the grating. We then set up equations to describe the optical path from A to B via P. This path length is then minimized according to Fermats principle and this will lead to a set of relations defining the imaging properties of the grating:

$$(\mathrm{AP})^2 = (x - \zeta y)^2 + (y - w)^2 + (z - l)^2,$$
$$(\mathrm{BP})^2 = (x' - \zeta)^2 + (y' - w)^2 + (z' - l)^2.$$

We then change co-ordinates and use the relation defining the surface of the grating:

$$x = r\cos\alpha \quad \text{and} \quad x' = r\cos\beta,$$
$$y = r\sin\alpha \quad \text{and} \quad y' = r'\sin\beta.$$

The equation for the grating surface is $(\zeta - R)^2 + w^2 + l^2 = R^2$.

The optical path $F = \mathrm{AP} + \mathrm{PB}$ should then be subject to Fermats principle and for an image both $\delta F/\delta w$ and $\delta F/\delta l$ should be zero for all values of w and l.

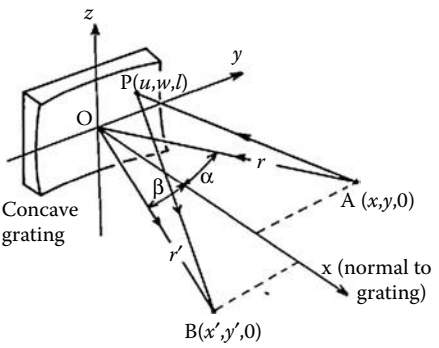

FIGURE 3.5
Schematic diagram of optical system.

However, it is not important in this case that all light paths from A to B are equal, but that all waves reaching B, from A, are in phase. For a grating, there is the possibility for different path lengths as there are reflections from very discrete areas, namely the grating rulings. This can be taken into account by allowing the light path to change by an integer number of wavelengths as w (the distance along the grating perpendicular to the grooves) changes by one grating ruling, that is,

$$F = \mathrm{AP} + \mathrm{PB} + \frac{wm\lambda}{a},$$

where m is the diffraction order, a the grating spacing (1/line density), and λ the wavelength.

Using the above relations, F can be written as a function of the variables $r, r', \alpha, \beta, \alpha', \beta', w$, and l.

The last part of the development requires F to be written as an expansion in various powers of w and l. The terms in the expansion can then be grouped together and useful relations can be obtained. There are a number of ways to do such an expansion but the one developed by Beutler in his 1945 paper leads to the most useful expressions. For a full derivation, the reader is directed to Beutlers paper.

Here $\mathrm{AP} = \Sigma F_i$ and $\mathrm{PB} = \Sigma F_{i'}$. The first two terms, that is, $i = 1$ and 2 will be

$$F_1 = r - w\sin\alpha,$$

$$F_2 = \frac{1}{2}w_2\left(\frac{\cos^2\alpha}{r} - \frac{\cos\alpha}{r}\right) + \text{higher-order terms},$$

$$F_1' = r' - w\sin\beta,$$

$$F_2' = \frac{1}{2}w_2\left(\frac{\cos^2\beta}{r'} - \frac{\cos\beta}{r}\right) + \text{higher-order terms}.$$

We can now examine the condition for a focus, that is, look at $\delta F/\delta w$ and $\delta F/\delta l = 0$ for all positions on the grating. Any deviation from zero will represent aberrations, which, in principle, can be calculated.

The first term gives

$$F_1 = r - w\sin\alpha + r' - w\sin\beta + \frac{wm\lambda}{a}.$$

If

$$\frac{\delta F}{\delta w} = \frac{\delta F}{\delta l} = 0,$$

then

$$-\sin\alpha - \sin\beta + \frac{m\lambda}{a} = 0.$$

This is nothing else, but the grating equation.

In the special case of plane gratings, $R = \infty$ and also $r = r' = \infty$, so the above equations are always zero and the only relation to think about is the grating equation and the plane grating cannot introduce any aberrations.

The grating equation tells in which direction an image at a given wavelength can be expected, but not where the focus will be. The position of the focus comes from the next order of the expansion.

$$F_2 = 0.5\,w^2\left(\frac{\cos^2\alpha}{r} - \frac{\cos\alpha}{R} + \frac{\cos^2\beta}{r'} - \frac{\cos\beta}{R}\right) + 0.5\,w^2\left(\frac{\sin\alpha}{r}\left(\frac{\cos^2\alpha}{r} - \frac{\cos\alpha}{R}\right) + \frac{\sin\beta}{r'}\left(\frac{\cos^2\beta}{r'} - \frac{\cos\beta}{R}\right)\right).$$

Now consider the first term and put its derivative w.r.t. w and l equal to 0. Again $\delta F/\delta l = 0$ by default. Then $\delta F/\delta w = 0$ implies either $w = 0$ or

$$\frac{\cos^2\alpha}{r} - \frac{\cos\alpha}{R} + \frac{\cos^2\beta}{r'} - \frac{\cos\beta}{R} = 0,$$

which leads to

$$\cos\alpha\left(\frac{\cos\alpha}{r} - \frac{1}{R}\right) + \cos\beta\left(\frac{\cos\beta}{r'} - \frac{1}{R}\right) = 0.$$

One solution to the above is given by $r = R\cos\alpha$ and $r' = R\cos\beta$.

If this solution is chosen, then even the higher-order terms in x.8 are zero. This solution represents a circle with radius $R/2$ and points on the circle are given by (r, α) and (r', β). This is the well-known Rowland circle. There are, of course, terms that depend on l and cross-terms that depend on both l and w that do not vanish and lead to aberrations. However, the overall imaging properties are not.

There is another useful solution to the above imaging equations. A second solution leads to the Wadsworth mounting as discussed in Section 3.7.2. The Wadsworth solution requires the light source to be at an infinite distance from the grating, that is, $r = \infty$, which can be represented by parallel light impinging on the grating. The image is then on the grating axis, that is, $\beta = 0$.

There are basically two types of spectrometers based on the Rowland circle. These operate in different wavelength regions, as discussed above, and are based on either normal or grazing incidence geometry. A discussion of these two types of instruments follows.

3.9 Normal Incidence Spectrometers

From the formulation above, it is clear that if an entrance slit is positioned on the Rowland circle, then the spectrum will also be imaged on the Rowland

circle. The image where the incidence angle equals the diffraction angle is the zeroth-order image, or mirror reflection ($\sin\alpha + \sin\beta = n\lambda/d$ and $n = 0$). This image contains light of all wavelengths and is often the strongest image produced by the spectrometer and hence a very useful calibration mark. We will mention this in more detail under the discussion of grating blaze angles. In principle, any position along the Rowland circle can be chosen for an entrance slit.

However, as with most optics, aberrations increase for off-axis imaging. Hence, if the incidence angle is kept small, the spectral image will not be distorted significantly by aberrations. In a classic design by Paul McPherson, the incidence angle was chosen to be 7.5°. Most commercial normal incidence spectrometers use this angle (or something very close) and unless the gratings are aberration-corrected, the opening angle is usually limited to less than $f/10$. Normal incidence instruments are relatively easy to construct and in the old days would have an entrance slit and a photographic plate bent to match the Rowland circle. In principle, a very wide wavelength range can be covered by a large enough plate, but in practice this would lead to problems with emulsions having different sensitivities for different wavelength regions. Also the geometrical size of such instruments can become very large, leading to problems of stabilities, and so on. The largest normal incidence instrument was built at the Argonne National Laboratory and had a diameter of 9 m. This geometry is not very convenient for using photoelectric detectors, such as photomultipliers, and so on. Hence the scanning design introduced by McPherson (see Figure 3.6) in 1963 made a huge impact on the usefulness of the normal incidence mounting.

Several other mountings for concave gratings are possible, as discussed in the book by Thorn et al. [15].

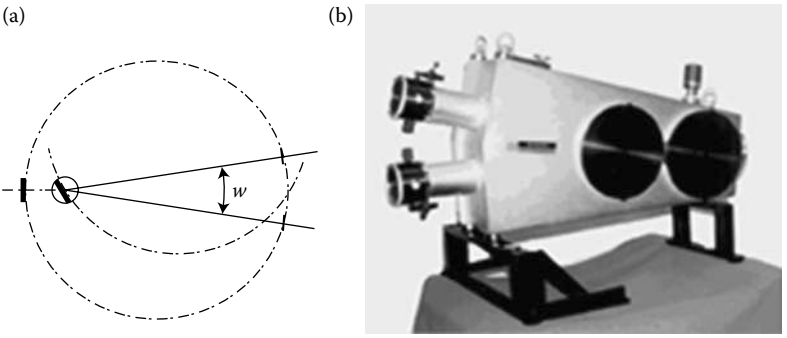

FIGURE 3.6
(a) shows schematically how by moving and rotating the grating the Rowland circle can be moved to keep the focus at the exit slit, and (b) shows how this leads to a much more compact spectrometer.

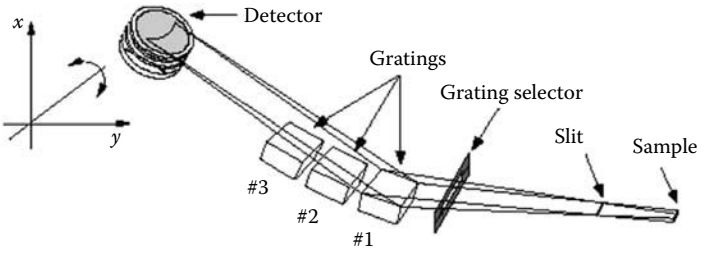

FIGURE 3.7
Layout of the optics.

3.10 Grazing Incidence Spectrometers

Grazing incidence spectrometers work exactly as one would imagine from the name, with the incident light falling at a very high (grazing) angle with respect to the grating. Typically this angle is between 85° and 89°, and the higher the angle, the better the reflectivity. One can then ask why not always use grazing incidence? The answer can be found above in the discussion on aberrations. As an example, we will consider the efficiency of a 1 m normal incidence spectrometer compared to a 1 m grazing incidence instrument.

Another classic problem with the grazing incidence geometry is clear from Figure 3.7, in which the angle of the detector to the incoming photons will also be grazing and lead to reflection off the detector surface. This can be a problem if, for example, a CCD detector is used in the image plane. A solution to this problem will be discussed in Section 3.12.2. A second problem associated more with grazing incidence spectrometers, although in principle it is a more general problem, is that of curved line shapes in the image plane (see Figure 3.7). This can, of course, be taken care of using software for any given spectrometer as the line curvature is known based on the exact geometry of the instrument.

3.11 What Influences the Efficiency of a Spectrometer?

The overall efficiency of a spectrometer is influenced by a number of effects/parameters, an example being the reflective properties of the optics. For wavelengths under 2000 Å, it is advised to minimize the number of reflections and optimally use only one. As said earlier, this is because the reflective properties of all materials drop rapidly for shorter wavelengths. The rapid drop in reflectivity can be combated by using the optic at a high incidence

angle. An illustration of this is shown in Figure 3.2 (GI-gold) where the reflectivity of gold is plotted as a function of incidence angle for a wavelength of 400 Å. One could then ask "why not always work using grazing incidence optics?" The answer, as indicated earlier, is that grazing optics suffer from large aberration properties and hence limit the light collection angles that can be used (see [11]). Hence it may well be that a normal incidence spectrometer can be more efficient than a grazing incidence spectrometer ever for quite short-wavelength light, indeed normal incidence spectrometers have been used down to around 250 Å.

A further influence on the efficiency of a spectrometer is the so-called grating blaze. Blaze will be explained below, however, if a grating is not blazed most of the diffracted light ends up in the zeroth-order, that is, the directly reflected light and hence contains no spectral information. Blaze is therefore defined as the concentration of a limited region of the spectrum into any order other than the zero order. Blazed gratings are manufactured to produce maximum efficiency at designated wavelengths. A grating may, therefore, be described as "blazed at 250 nm" or "blazed at 1 μm," etc., by appropriate selection of groove geometry.

The blaze condition is achieved by controlling the groove shape to be right-angled triangles, as shown in Figure 3.8. The groove profile is most often calculated for under the Littrow condition for reflection, that is, the input and output rays propagate along the same axis:

$$\sin\alpha + \sin\beta = \frac{n\lambda}{d}.$$

However when blazed, $\alpha = \beta = \omega$, where ω is the blaze angle.

Hence, $2\sin\omega = n\lambda/d$ gives the blaze angle.

As a general approximation, for blazed gratings the strength of a signal is reduced by 50% at two-thirds the blaze wavelength, and 1.8 times the blaze wavelength.

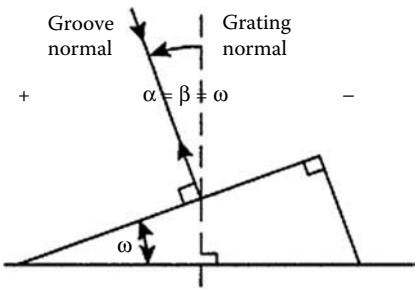

FIGURE 3.8
The principle of the grating blaze angle.

3.11.1 Aside

A major break through in grating design/manufacture occurred in the early 1980s. This was the invention of variable-spacing gratings. Such gratings could lead to flat-field spectral imaging and combined with the soon-to-be developed CCD and multichannel plate detectors has led to very powerful spectrometers of particular interest at synchrotron facilities. This breakthrough will be described below.

3.12 The Aberration-Corrected Flat-Field Spectrograph

Based on their development of numerically controlled ruling engines, in the early 1980s, Harada and Kita reported the availability of mechanically ruled aberration-corrected concave gratings, which are still widely used in vacuum ultraviolet spectroscopy nowadays.

The discussion below follows the work of Harada et al. from the early 1980s.

3.12.1 Principles of Flat-Field Spectrograph

For any spectrograph, the diffracted light varies with wavelength following the so-called grating equation:

$$\sin\alpha + \sin\beta = \frac{m\lambda}{d}.$$

If the groove spacing d is constant, for a given wavelength λ and diffraction order m, the angle of diffraction β is determined only by the angle of incidence α. If the slit of the spectrograph and the grating is placed on the Rowland circle, whose diameter is equal to the radius of curvature of the grating surface, then the diffracted light has to fall on the Rowland circle, as shown in Figure 3.9a. However, if the groove spacing varies, which is true in mechanically ruled aberration-corrected concave gratings, the angle of diffraction β now depends both on the angle of incidence α and the groove spacing d. So the angle of diffraction β can be regulated through proper ruling of the grooves. Through proper design of the groove spacing, aberration-corrected concave gratings can be made, as shown in Figure 3.9b.

3.12.2 Design of Aberration-Corrected Concave Gratings through Fermat's Principle

Figure 3.10 shows a typical optical set up of a grazing incidence flat field spectrometer. As shown in Figure 3.5, the light emitting from $A(x, y, 0)$ is diffracted at $P(u, w, l)$ and focused at $B(x', y', 0)$. The light path function F can be expessed by

$$F = \langle AP\rangle + \langle PB\rangle + nm\lambda.$$

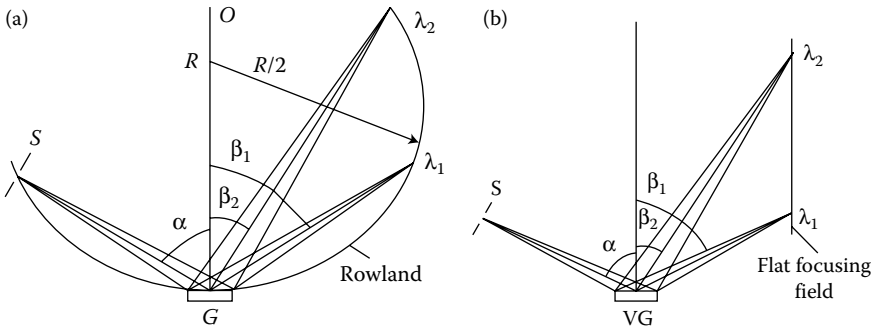

FIGURE 3.9
Concave gratings with (a) invariable and (b) variable line space.

The above equation can be derived following the throught that the light diffracted at two adjacent grooves is enhanced only when the light path difference equals $m\lambda$. And n is the groove number counted from the center of the grating.

According to Fermat's principle, the real light path has to satisfy

$$\frac{\partial F}{\partial w} = 0 \quad \text{and} \quad \frac{\partial F}{\partial l} = 0.$$

In the papers [17,18], the authors used a simpler way to rule the grating, which in contrast to their 1980 ruling process, in which aside from the groove spacing they also included the groove tilting angle θ [16]. In the following discussion, only the groove spacing varies, and the tilting angle is always zero.

The variation of the groove spacing is defined as

$$\sigma = \frac{\sigma_0}{1 + (2b_2/R)w + (3b_3/R^2)w^2 + (4b_4/R^3)w^3 + \cdots},$$

where σ_0 is the nominal spacing of the grooves, or the groove spacing at the center of the grating. B_j $(j = 2, 3, 4, \ldots)$ are the ruling parameters.

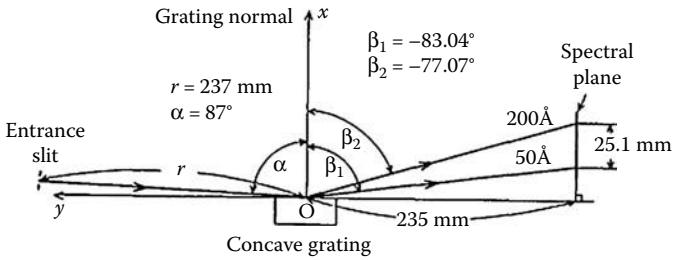

FIGURE 3.10
Schematic and design specifications for the flat-field spectrograph using a mechanically ruled aberration-corrected concave grating: 1200 groves/mm; $R = 5649$ mm; 50×30 mm^2 ruled area.

Combining the above several equations, the light path function as a power series of w and l can be expressed as

$$F = r + r' + wF_{10} + w^2F_{20} + l^2F_{02} + w^3F_{30} + wl^2F_{12} + w^4F_{40} + w^2l^2F_{22} + l^4F_{04} + T(w^5).$$

In the above equation, every F_{ij} term can be expressed by the term $F_{ij} = C_{ij} + (m\lambda/\sigma_0)M_{ij}$.

For the detailed expression of each term, C_{ij} and M_{ij}, please refer to the literature [16]. In general, C_{ij} is the term corresponding to the conventional grating, M_{ij} is the term arising from the varied spacing grooves. F_{10} is related to the dispersion of the grating, F_{20} to the horizontal focal condition, F_{02} to astigmatism, F_{30} to coma-type aberration, and other F_{ij} term to higher-order aberrations.

To achieve completely stigmatic image focusing, the condition $F_{ij} = 0$ have to be satisfied. However, it is impossible to satisfy the stigmatic condition for the total wavelength range in which the grating is used, so in practical design one only needs to make the key term of F_{ij} zero or minimum.

We can obtain, for example, for $F_{10} = 0$ and $F_{20} = 0$,

$$r' = \frac{rR\cos^2\beta}{r[\cos\alpha + \cos\beta - 2(\sin\alpha + \sin\beta)b_2] - R\cos^2\alpha}.$$

When some of the grating and mounting parameters such as σ_0, α, r, and the position of the flat detector surface are predetermined, the above equation which gives the combination of R and b_2 will minimize the deviation between the horizontal focal curve $F_{20} = 0$ and the detector plane within the diffraction domain of β. Coma and spherical aberrations can be reduced by choice of proper values of b_3 and b_4 to minimize the values of F_{30} and F_{40}, respectively, within the diffraction domain of β.

Acknowledgment

Many of the ideas presented in this chapter are based on a compendium called "Spectroscopiska Instrument" written in Swedish by Professor Ulf Litzen, Lunds Universitet, Reprocentralen, in 1985. We are very grateful for his co-operation in this current project.

References

1. P. Beierersdorfer et al., *Phys Rev. A* 64, 032506, 2001.
2. P. Doschek, in *Autoionization*, edited by A. Temkin. New York: Plenum Press, 1985, pp. 171–256.

3. B. Edlén, *Mon. Not. R. Astron. Soc.* 105, 323, 1945.
4. A. E. Kramida, A. N. Ryabtsev, J. O. Ekberg, I. Kink, S. Mannervik, and I. Martinson, *Phys. Scripta* 78, 025302, 2008.
5. B. Edlén and P. Swings, *Astrophys. J.* 95, 532, 1942.
6. *XOP X-ray Software*. European Synchrotron Radiation Facility. http://www.esrf.eu/computing/scientific/xop2.1/
7. McPherson, Inc. http://www.mcphersoninc.com/
8. G. R. Harrison, *Proc. Am. Phil. Soc.* 102(5), 483–491, 1958.
9. Jobin Yvon. http://www.horiba.com/scientific/products/optics-tutorial/diffraction-gratings/
10. L. Seidel, *Astr. Nach.* 1856, 289, 1840.
11. J. E. Mack, J. R. Stehn, and B. Edlén, *J. Opt. Soc. Am*. 22, 245, 1932.
12. W. Welford, *Aberrations of Optical Systems*. Taylor & Francis, 1986.
13. J. A. Samson and D. L. Ederer, *Vacuum Ultraviolet Spectroscopy II, Vol. 32 in Experimental Methods in the Physical Sciences*. San Diego, CA: Academic Press, 1998. ISBN 0-12-475979-30.
14. H. G. Beutler, *J. Opt. Soc. Am.* 35, 311 1945.
15. A. Thorn, U. Litzen, and S. Johansson, Spectrophysics, Principles and Applications. Berlin, Heidelberg, New York: Springer, 1999. ISBN 3-540-65117-9.
16. T. Harada and T. Kita, *Appl. Opt.* 19(23), 3987, 1980.
17. T. Kita et al., *Appl. Opt*. 22(4), 512, 1983.
18. T. Harada et al., *Appl. Opt*. 38(13), 2743, 1999.